

Electrically detected magnetic resonance of two-dimensional electron gases in Si/SiGe heterostructures

C. F. O. Graeff*

Departamento de Física e Matemática, FFCLRP-USP, Av. Bandeirantes 3900, 14040-901 Ribeirão Preto, Brazil

M. S. Brandt, M. Stutzmann, M. Holzmann, and G. Abstreiter

Walter Schottky Institut, Technische Universität München, Am Coulombwall, D-85748 Garching, Germany

F. Schäffler

Institut für Halbleiterphysik, Johannes Kepler Universität Linz, A-4040 Linz, Austria

(Received 4 September 1998)

Strained Si/Si_{0.75}Ge_{0.25} heterostructures, grown by solid source *e*-beam evaporation molecular-beam epitaxy on Si(100) substrates, have been studied by electrically detected magnetic resonance. Samples with a low-temperature mobility of about 10⁵ cm²/V s were used, some with Schottky gates enabling control of the electron density in the channel. For $T < 50$ K, a conduction-band electron-spin-resonance signal caused by electron-electron scattering in the two-dimensional channel was observed in the dark. The signal intensity, *g* factor, and linewidth were observed to depend on electron density n_e and magnetic-field orientation. For $n_e = 4 \times 10^{11}$ cm⁻², $g_{\parallel} = 2.0007$ (H parallel to the major conduction-band valley axis), and $g_{\perp} = 1.9999$ (H perpendicular to major axis), which leads to an anisotropy of $g_{\parallel} - g_{\perp} = (8 \pm 2) \times 10^{-4}$. For $n_e < 3 \times 10^{11}$ cm⁻², the anisotropy nearly disappears. For $H \parallel [100]$, resonance linewidths as low as 70 mG are observed. A model for the resonant change in the conductivity is developed and compared to experiment. [S0163-1829(99)03420-7]

I. INTRODUCTION

Quantum-confined electron systems are of particular interest in basic and applied semiconductor physics. Most of the experiments made on low-dimensional semiconductors have been performed in Si MOSFET's (metal-oxide-semiconductor field-effect transistors) and in GaAs/Al_{1-x}Ga_xAs heterostructures. In the last decade, strong interest also arose in the study of Si/SiGe heterostructures,¹⁻⁴ with the motivation to improve electron and hole mobility for higher performance Si-based devices. As an example, the electron mobility achieved in such heterostructures is about one order of magnitude larger than in silicon MOSFET's.⁵

The electron *g* tensor is one of the basic parameters in semiconductors. It describes the deviation of the electronic *g* value in a solid from that of a free electron caused by the spin-orbit interaction. Accurate experimental measurements of the *g* tensor therefore can provide a sensitive test for band-structure calculations. Unfortunately, the spin resonance (ESR) of electrons in quantized systems is rarely observed directly.⁶⁻⁹ For Si/SiC heterostructures, direct ESR measurements have been reported.⁷ However, these authors did not observe the expected anisotropy of the *g* tensor. Their assignment of the observed ESR signal to a two-dimensional (2D) electron gas is largely based on the specific temperature dependence of the Pauli-type magnetization observed in this case. More recently, direct ESR measurements of Si/SiGe heterostructures yielded peak-to-peak resonance linewidths as low as $\Delta H_{pp} = 70$ mG,^{8,9} compared to the linewidths of several G observed earlier. Since the sensitivity of conventional ESR is proportional to ΔH_{pp}^{-2} , such narrow resonances

are an important factor for the detection of ESR from two-dimensional electron gases with conventional ESR experiments.

Instead of resonant methods, nonresonant techniques like magnetotransport are commonly used to study *g* factors. However, in many cases these nonresonant techniques lack the necessary accuracy in the determination of the *g* factor, and require the use of strong magnetic fields. In contrast, comparatively little has been done both experimentally and theoretically in the last decades on the physics of quasi-low-dimensional electron gases at low magnetic fields.

In order to overcome the difficulties of conventional ESR in measuring low-dimensional electron-gas systems, in particular the small amount of spins present in the samples, indirect detection of ESR has been used. GaAs/Al_{1-x}Ga_xAs heterostructures were the first semiconductor materials in which the spin resonance of a 2D electron gas was studied, using bolometric detection.¹⁰ Optically detected magnetic resonance (ODMR) has been successfully used to study both type-I and type-II quantum wells.¹¹⁻¹⁵ In Si/SiGe superlattices, an isotropic resonance at $g = 1.9986$ has been attributed to conduction electrons.^{13,14}

The electrical analog of ODMR and the method applied here to the study of the spin properties of 2D electron gases is electrically detected magnetic resonance (EDMR). This method has been widely used for the investigation of recombination, trapping, and tunneling transitions in amorphous and crystalline semiconductors.¹⁶⁻²³ In an EDMR experiment, microwave-induced resonant changes in the conductivity are measured as the sample is subjected to a slowly swept dc magnetic field. A particular advantage of this experimental method is its much higher (by up to a factor of 10⁸) sensitivity to paramagnetic states participating in charge

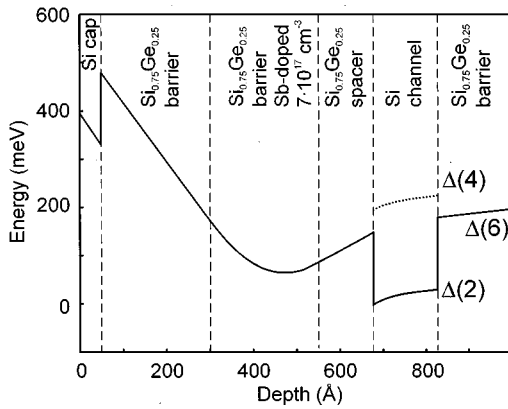


FIG. 1. Schematic diagram of the conduction band of the Si/SiGe heterostructures studied in this work. $\Delta(n)$ indicates the degeneracy of the conduction-band minima in the unstrained and strained layers.

transport,²¹ thus allowing their microscopic identification. The first electrical detection of ESR on a 2D inversion layer was reported in a Si MOSFET.²² The authors attributed resonances observed with an isotropic g factor of 2.000 to spin-dependent scattering of conduction electrons by neutral impurities, as evidenced by hyperfine split EDMR lines characteristic of phosphorous dopants in crystalline silicon.

In the present work we extend the use of EDMR to the study of the spin properties of electrons in a transfer-doped strained Si/SiGe heterostructure. As shown by the increased mobility of the 2D electron gas in a Si/SiGe heterostructure, the scattering, in particular due to neutral dopants and impurities, is reduced so that a significant narrowing of the resonance lines is achieved compared to earlier work. This enables us to observe the expected g -factor anisotropy in a silicon 2D electron gas. The exact dependence of the EDMR signal amplitude on the electron density in the 2D gas allows us to assign the underlying spin-dependent process to electron-electron scattering in the 2D electron gas.

II. EXPERIMENTAL DETAILS

The Si/Si_{0.75}Ge_{0.25} heterostructure studied here was grown by solid source e -beam evaporation molecular-beam epitaxy on weakly p -type Si(100) substrates. The layer sequence of structure C936 is shown in Fig. 1. Transfer doping is achieved by an antimony δ -doping layer separated from the 2D channel by approximately 10 nm. The samples were lithographically structured in order to form a Hall-bar mesa. Ohmic contacts to the 2D channel were made in two stages: first, antimony and gold were evaporated and alloyed in using a rapid thermal anneal, then titanium and gold were evaporated for contact reinforcement. In addition to the Ohmic contacts, some samples had an evaporated Pd Schottky barrier gate contact.

The electron sheet density n_e and the electron mobility μ were deduced from low-temperature Hall-effect measurements.¹ For samples without gate, n_e was typically $4 \times 10^{11} \text{ cm}^{-2}$, with μ around $9 \times 10^4 \text{ cm}^2 \text{ V}^{-1} \text{ s}^{-1}$ at 4.2 K. In samples equipped with a top gate, n_e showed a linear dependence on the gate voltage and could be changed typically from 1×10^{11} to $7 \times 10^{11} \text{ cm}^{-2}$, for gate voltages be-

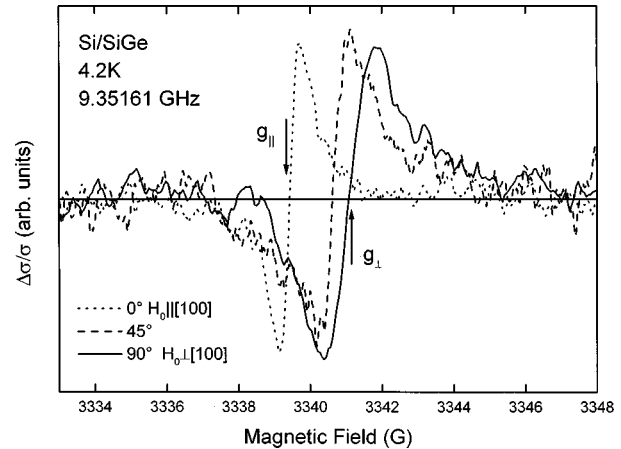


FIG. 2. Typical electrically detected magnetic spin resonance (EDMR) signals for a sample without gate under different orientations of the sample growth direction with respect to the magnetic field H_0 .

tween 0 and 900 mV. The corresponding electron mobility varied as a function of the electron density between 20 000 and $180\,000 \text{ cm}^2 \text{ V}^{-1} \text{ s}^{-1}$ ($\mu \propto n_e^{2.44}$).²⁴ This strong dependence of the channel mobility on carrier density is indicative of weak localization in potential fluctuations for low electron densities.

The EDMR measurements were made with an X-band ESR spectrometer (Bruker ESP300), using a standard rectangular resonator (TE₁₀₂ mode) and a helium-flow cryostat. The resonant conductivity changes were measured as a function of the magnetic field, using magnetic-field modulation and phase-sensitive detection. The measurements were typically performed between 4.2 and 25 K. Diphenyl- β -picrylhydrazyl (DPPH) ($g=2.0036$) and bulk silicon doped with $1 \times 10^{18} \text{ cm}^{-3}$ phosphorous ($g=1.9987$) were used as g -factor references. The use of P-doped Si as a reference material is useful to ensure an exact comparison of the g factors between bulk and 2D electrons in silicon. Since typical g -factor changes in our measurements were on the order of 10^{-4} , several precautions were taken in order to guarantee the precision of the g -factor determination, such as calibration by the reference samples before and after each sequence of measurements and employment of field-frequency-locking to a DPPH g -value standard in an external cavity, especially when very narrow resonance lines were investigated.

III. RESULTS

A. Si/SiGe without gate

In Fig. 2, typical EDMR spectra of a Si/Si_{0.75}Ge_{0.25} heterostructure without gate are shown as a function of the relative orientation of the external magnetic field H_0 with respect to the sample growth direction [100]. An angle of 0° thus corresponds to $H_0 \parallel [100]$, and an angle of 90° to $H_0 \perp [100]$. The signal amplitude has been normalized. Upon rotation of the sample, the resonance frequency of the microwave resonator changes slightly. For better comparison, the spectra shown have been corrected to the microwave frequency of the 0° measurement. As can be seen, the signal observed has a clear anisotropy of the effective g factor (cal-

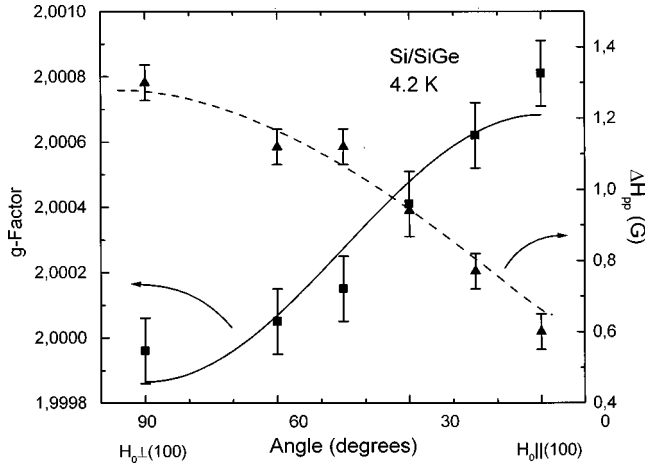


FIG. 3. g factor (full line) and linewidth ΔH_{pp} (dashed line) as a function of the relative orientation between the magnetic field H_0 and the sample growth direction. The fit of the g -factor anisotropy was done using Eq. (1). The clear anisotropy indicates that only electrons in the conduction-band valleys with the long axis parallel to the sample growth direction [100] contribute to the spin-dependent transport path. The dashed line is a guide to the eye.

culated from the ratio of the microwave frequency and the magnetic field at the zero crossing point of the spectrum) as well as a corresponding anisotropy of the peak-to-peak linewidth ΔH_{pp} .

The origin of the anisotropy is the strain-induced splitting of the conduction-band valleys. The tensile strain in the Si layer sandwiched between the SiGe layers lifts the degeneracy of the six silicon conduction-band valleys of bulk silicon. As a consequence, and as shown in Fig. 1, the two Si conduction-band valleys with their major axis parallel to the [100] growth direction have a conduction-band energy minimum $\Delta(2)$ lower than the conduction-band minimum of the SiGe layer $\Delta(6)$, while the other four valleys of the strained Si layer (with major axes parallel to [010] or [001]) have a higher energy, $\Delta(4)$. In the present case, the electron confinement energy in the silicon quantum well is approximately 160 meV.^{25,26}

Since the g tensor is determined by the spin-orbit interaction and the orbital momentum of an electron in a Si valley, it should be different if the motion of the electron is parallel or perpendicular to the major valley axis. Indeed, when the valley degeneracy is lifted due to uniaxial strain, an anisotropic g tensor is observed in heavily doped bulk Si.²⁷ For an axially symmetric g tensor with the main components g_{\parallel} and g_{\perp} , the orientation dependent g factor is given by

$$g^2 = g_{\parallel}^2 \cos^2 \theta + g_{\perp}^2 \sin^2 \theta, \quad (1)$$

where θ is the angle between the applied field H_0 and the major valley axis (parallel to [100]). From a least-square fit to the g -value anisotropy observed for the Si/SiGe heterostructure (Fig. 3), g_{\parallel} is found to be 2.0007 ± 0.0001 and $g_{\perp} = 1.9999 \pm 0.0001$, which leads to a dispersion $\Delta g = g_{\parallel} - g_{\perp} = (8 \pm 2) \times 10^{-4}$. This value for Δg is in good agreement with experimental results for doped Si under uniaxial stress by Wilson and Feher,²⁷ who determined $\Delta g = (11 \pm 1) \times 10^{-4}$ for the case of complete repopulation into the $\Delta(2)$ valleys. It should be noted, however, that these authors de-

duced their value of Δg via extrapolation from g -factor shifts observed under small applied strains ($\leq 0.1\%$). In the present case, only the $\Delta(2)$ valleys are occupied, and the anisotropy can be observed without need for further extrapolation. Based on this quantitative agreement, it can therefore be concluded that the EDMR signal observed here indeed arises from electrons in the two conduction-band valleys parallel to [100], as expected for a quasi-2D electron gas.

Using the above values for g_{\parallel} and g_{\perp} , we note that the average g factor g_{ce} of the conduction electrons in the quasi-2D Si channel, which is calculated according to

$$g_{ce} = \frac{1}{3} g_{\parallel} + \frac{2}{3} g_{\perp}, \quad (2)$$

is obtained as $g_{ce} = 2.0002 \pm 0.0001$, compared to literature values of 1.99875 ± 0.00010 obtained in heavily P-doped bulk Si,²⁸ and 1.9993 ± 0.0001 found in Si/SiC multiple quantum wells.⁷ We will address this difference in our discussion below. For the calculation of the g factors, we use $h = 6.626075 \times 10^{-34}$ J s and $\mu_B = 9.274015 \times 10^{-24}$ J/T.²⁹

As also shown in Fig. 3, the peak-to-peak linewidth ΔH_{pp} is found to decrease from approximately 1.30 ± 0.05 to 0.60 ± 0.05 G for H_0 perpendicular and parallel to [100], respectively. The line shape is compatible with a Lorentzian, which is characteristic for homogeneous broadening. For homogeneous lines, the spin-spin relaxation time T_2 can be calculated by³⁰

$$T_2 = \frac{2}{\sqrt{3}} \frac{\hbar}{g \mu_B} \frac{1}{\Delta H_{pp}^0}, \quad (3)$$

where ΔH_{pp}^0 is the linewidth in the unsaturated case. According to this expression, T_2 is varying in our samples from 5×10^{-8} to 1×10^{-7} s. The spin-lattice relaxation time T_1 can be determined from the saturation behavior of the EDMR line. Again with the assumption of homogeneous broadening, the EDMR peak-to-peak amplitude $(\Delta \sigma / \sigma)_{pp} = y'_m$ of the first derivative signal obtained by magnetic-field modulation is

$$\Delta \sigma / \sigma = y'_m \propto \frac{H_1^2}{\left[1 + \left(\frac{g \mu_B}{\hbar} \right)^2 H_1^2 T_1 T_2 \right]^{3/2}}, \quad (4)$$

where H_1 is the microwave magnetic field.³⁰ Note that the EDMR signal intensity is proportional to the absorbed microwave power, $\chi'' H_1^2$, in contrast to conventional ESR, where the signal intensity is proportional to the magnetization, $\chi' H_1$. The dependence of H_1 on the microwave power has been determined experimentally by electron-nuclear double resonance (ENDOR) measurements,³¹ and is in accordance with theoretical estimates.³⁰ A fit of Eq. (4) to the observed power dependence of the EDMR signal is shown in Fig. 4. Using the above value for T_2 , we obtain $T_1 = (1.0 \pm 0.3) \times 10^{-5}$ s. The power broadening of the resonance line, which can also be used for the determination of $T_1 T_2$, is included in Fig. 4. The fact that both line-shape broadening and the power dependence of the signal intensity give the same value for $T_1 T_2$ provides further evidence of the assumption of homogeneous broadening.

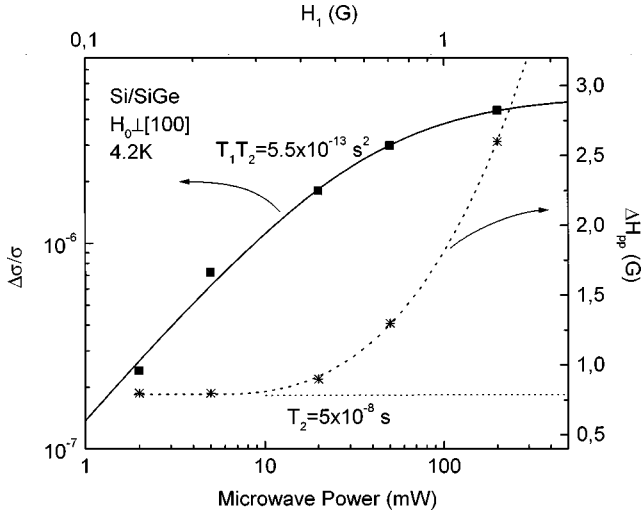


FIG. 4. Microwave power dependence of the EDMR signal amplitude $\Delta\sigma/\sigma$ (full line) and of the linewidth ΔH_{pp} (dotted line). The fit of $\Delta\sigma/\sigma$ was done according to Eq. (4).

B. Si/SiGe with a Pd gate

We now turn to an investigation of the influence of the electron sheet density n_e on the EDMR properties. In Fig. 5, the effect of varying n_e in Si/SiGe heterostructures equipped with a top gate is shown for $H_0 \perp [100]$. An increase of n_e leads to a shift in the g factor as well as a change in the line shape. For low n_e , the g -factor anisotropy is not as pronounced as for samples with high n_e as shown in Fig. 6. In fact, g_{\perp} varies continuously from 2.0005 ± 0.0001 to 1.9994 ± 0.0001 for n_e varying from 1×10^{11} to $7 \times 10^{11} \text{ cm}^{-2}$, while g_{\parallel} is basically unaffected by n_e with $2.0006 < g_{\parallel} < 2.0007$ (Fig. 7).

Finally, Fig. 8 shows the linewidth ΔH_{pp} as a function of the magnetic-field orientation for two different n_e 's. For low n_e and $H_0 \parallel [100]$, ΔH_{pp} can be as small as $70 \pm 5 \text{ mG}$. Note that the magnetic-field orientation dependence for different n_e follows more or less the same trend.

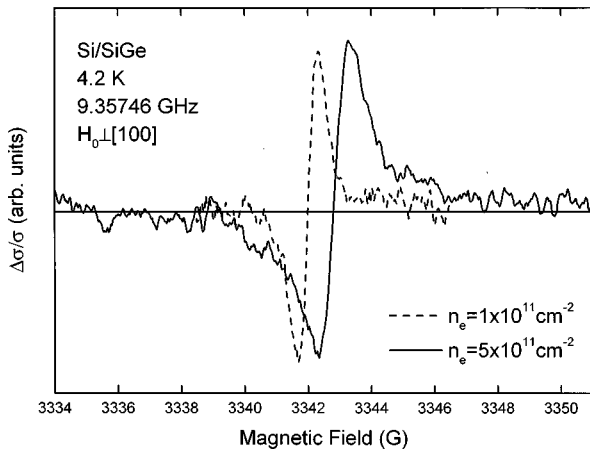


FIG. 5. EDMR signals for a sample with gate, at different electron densities n_e in the channel.

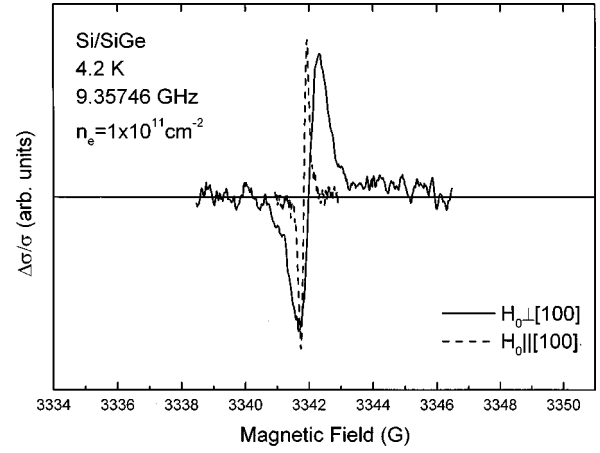


FIG. 6. Anisotropy of the EDMR signal for a sample with gate, and $n_e = 1 \times 10^{11} \text{ cm}^{-2}$.

IV. DISCUSSION

A. Origin of the EDMR signal

From the features presented in Sec. III, most prominently the observed absolute value of g_{ce} plus the fact that the anisotropy of the g factor agrees quantitatively with earlier results for conduction electrons in strained silicon, the EDMR signal observed here is assigned to the quasi-2D electron gas formed in the Si quantum well. However, the exact spin-dependent process leading to the observed resonant changes of the conductivity remains to be identified. In the case of dark conductivity, electron-electron scattering, scattering at impurities or defects, or tunneling are the potential spin-dependent processes.

Long-range impurity scattering is found to be the dominant relaxation mechanism in these samples, since the transport relaxation time τ_r exceeds the single-particle relaxation τ_s by at least a factor of 10 (Ref. 1). However, we note that only neutral (paramagnetic) impurities would give rise to an EDMR signal, since only the scattering of two spins is spin dependent. In contrast to the MOSFET's studied by Gosh and Silsbee,²² in which scattering with the background phosphorous dopants was observed, the dominant paramagnetic species in Si/SiGe heterostructures are the remaining neutral Sb dopants in the SiGe barrier, with a distance of about 10

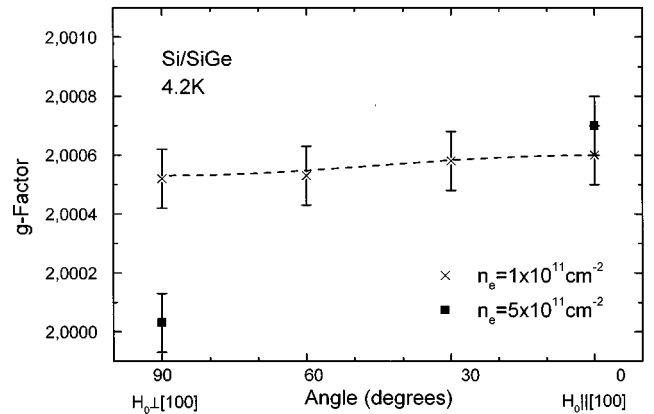


FIG. 7. Anisotropy of the g factor for different electron densities n_e in the channel. The line is a fit to Eq. (1).

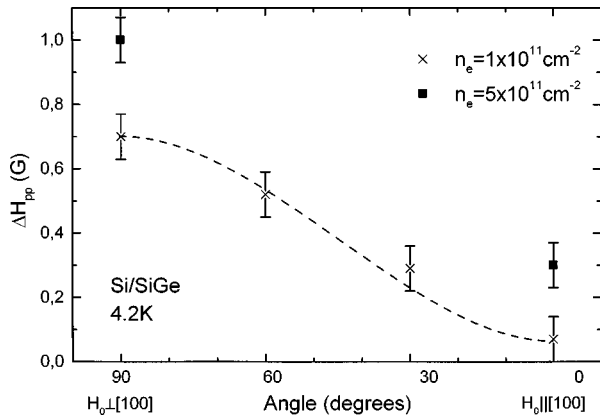


FIG. 8. Linewidth ΔH_{pp} as a function of the sample orientation with respect to the magnetic field H_0 for different electron densities n_e in the channel. The line is a guide to the eye.

nm to the edge of the Si channel. The effective range of a scattering potential for electrons at neutral dopants can be estimated from the radius of the outer electron in a negatively charged hydrogen atom, H^- . This radius has been found to be about 2.1 Bohr radii.³² Estimating the Bohr radius of $Sb:Si_{0.75}Ge_{0.25}$ within the effective-mass approximation, we obtain an effective scattering range for electrons at antimony dopants in the barrier of 2–5 nm. This effective scattering range is at least a factor of 2 smaller than the distance between the Sb doping layer and the Si channel, thus making the scattering probability very small. In addition, the g factor of shallow donors in $Si_{0.75}Ge_{0.25}$ should be quite different from the g factors observed here,²⁸ due to the much stronger spin-orbit coupling of Ge (Ref. 33). Although to our knowledge experimental g values have not been determined systematically in Si-Ge alloys, it is reasonable to expect a strong modification of the g values for a Ge content of 30% (cf. the extensive work on ESR in amorphous hydrogenated Si-Ge alloys^{23,34,35}). Most important, however, is the fact that in the particular heterostructure studied (C936), it is known that no neutral dopants remain in the doping layer, and that the carriers not transferred into the Si channel are in the cap layer. We can therefore completely exclude contributions of neutral dopant scattering to the observed spin-dependent signal.

Similar arguments concerning the g factor can be used to discard scattering at or tunneling to localized defects as the spin-dependent mechanism. Thus we note the complete absence of an EDMR signal with a g factor close to that of defects at Si interfaces or surfaces, which typically have $g_{\parallel} \approx 2.0015$ and $g_{\perp} \approx 2.0085$ (Ref. 36). An example of such a defect-related EDMR signal was observable in the present samples only at higher temperatures (above 50 K) and under bias illumination. For comparison, such an anisotropic defect-related EDMR spectrum is shown in Fig. 9. The line shape and the g values (about 2.004) are visibly different from what is observed for conduction electrons in the Si quantum well. The exact location of the defects leading to this EDMR response has not been identified yet, but an obvious origin would be the Si cap layer used to protect the transfer doping layer sequence. Since defect related signals are not the topic of the present paper, we refrain from a further discussion.

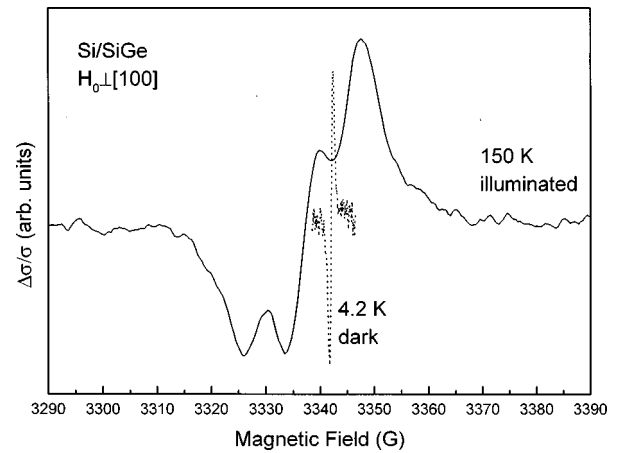


FIG. 9. Comparison of the electrically detected magnetic resonance of the Si/SiGe heterostructure under illumination at 150 K (straight line) and in the dark at 4.2 K (dotted line). g factor, and linewidth of the spectrum under illumination are typical for defects in silicon.

Additional evidence for electron-electron scattering in the 2D electron gas as the origin of the EDMR signals comes from the dependence of the signal amplitude $\Delta\sigma/\sigma$ on n_e . In Fig. 10, $\Delta\sigma/\sigma$ is plotted as a function of n_e for $H_0 \perp [100]$. As already evident from Fig. 8, a significant change in the linewidth occurs as a function of n_e , in addition to a change in the signal amplitude. For a correct analysis of the signal intensity, this broadening has to be taken into account. Therefore, the data in Fig. 10 show the peak-to-peak EDMR signal amplitude $\Delta\sigma/\sigma_{pp}$ for a magnetic-field modulation amplitude of $\Delta H_{mod} = 1/2\Delta H_{pp}$ which corresponds to the maximum EDMR amplitude obtained in a corresponding experiment using microwave power modulation. The corresponding data for $H_0 \parallel [100]$ show an identical behavior.

To understand the explicit dependence of the EDMR amplitude on the electron sheet density, we use a modified version of a model originally developed by Ghosh and Silsbee for the case of a Si MOSFET's (Ref. 22) based on concepts

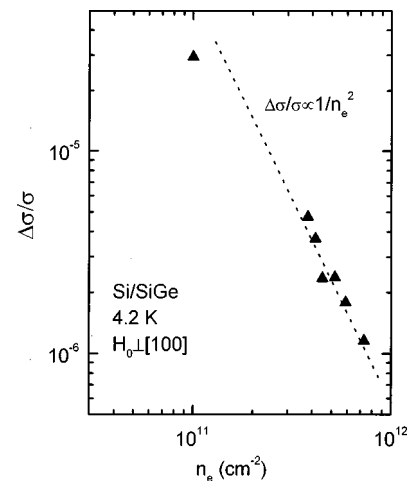


FIG. 10. EDMR signal amplitude as a function of electron density n_e in the channel for a microwave power of 10 mW corresponding to $H_1 = 0.3$ G. The $1/n_e^2$ dependence of $\Delta\sigma/\sigma$ is a clear indication that electron-electron scattering in the quasi-2D channel is the dominant spin-dependent process.

going back to the pioneering work of Schmidt, Solomon,¹⁶ and Honig.¹⁷ In this model, it is assumed that the electron-electron scattering cross section Σ depends on the relative orientation of the spins in such a way that the scattering cross section of a pair of electrons forming a triplet (total spin $S = 1$) is different from the cross section of a pair forming a singlet ($S = 0$) state. The presence of a magnetic field polarizes the conduction-electron spin system, increasing the relative population of triplet states. The total conduction-electron cross section Σ can be written in terms of the spin polarization p and the singlet and triplet scattering cross sections Σ_s and Σ_t , respectively:

$$\Sigma = \Sigma_0(1 - \beta p^2), \quad (5)$$

where $\Sigma_0 \equiv (\Sigma_s + 3\Sigma_t)/4$, and $\beta \equiv (\Sigma_s - \Sigma_t)/(\Sigma_s + 3\Sigma_t)$. The conduction electrons in the Si channel are best described as a two-dimensional degenerate Fermi gas with an equilibrium spin polarization given by

$$p = \frac{g \mu_B H_0}{2(E_F - E_0)}, \quad (6)$$

where E_F is the Fermi level and E_0 is the bottom of the first subband. Under spin resonance, this polarization is reduced by a factor of $(1 - s_e)$, where $0 \leq s_e \leq 1$ is the saturation parameter, with $s_e = 1$ corresponding to complete saturation.

The electron-electron scattering rate $1/\tau_e$ (Refs. 37 and 38) is a function of Σ , and, to first order, a relative variation of Σ will result in an equal and opposite relative variation of τ_e : $\Delta\tau_e/\tau_e = -\Delta\Sigma/\Sigma$. Equation (5) shows that a variation in Σ can be induced by a change of the spin polarization of the carriers. This can be achieved by applying a resonant field as in the case of an electron-spin-resonance experiment. A resonant microwave field induces transitions between the Zeeman spin levels, randomizing the populations of triplet and singlet states. Hence the spin polarization of the system is reduced, and, for high microwave powers, when the induced spin-flip rate becomes larger than the spontaneous relaxation rate, the polarization vanishes. For small variations $\Delta\sigma$ of the conductivity σ ,

$$\frac{\Delta\sigma}{\sigma} \cong -\beta p^2 [1 - (1 - s_e)^2] \frac{1/\tau_e}{1/\tau_t} \quad (7)$$

has been predicted for the normalized EDMR amplitude,²² where τ_t is the transport relaxation time. When only the lowest subband is occupied,

$$n_e = \frac{\nu m^*}{\pi \hbar^2} (E_F - E_0), \quad (8)$$

where ν is the valley degeneracy factor (in our case $\nu = 2$). Combining Eqs. (6) and (8) and substituting in Eq. (7), we obtain

$$\frac{\Delta\sigma}{\sigma} \cong -\beta \left(\frac{g \mu_B H_0 m^*}{n_e \pi \hbar^2} \right)^2 [1 - (1 - s_e)^2] \frac{1/\tau_e}{1/\tau_t}. \quad (9)$$

Neglecting implicit dependencies of τ_e , τ_t , and β on temperature T or n_e , we would like to point out that the explicit dependencies of Eq. (9) on these experimental parameters differ markedly from those which are obtained

when $\Delta\sigma/\sigma$ is estimated for electron-electron scattering in bulk semiconductors. While for quasi-2D electron gases $\Delta\sigma/\sigma$ is predicted to be proportional to $1/n_e^2$ and to be independent of T , the situation is reversed for the case of 3D gases, where $\Delta\sigma/\sigma$ is expected to be proportional to $1/T^2$ and to be independent of the electron concentration. Indeed, the $1/n_e^2$ dependence of $\Delta\sigma/\sigma$ for a 2D electron gas is clearly observed in Fig. 10. Additional measurements on samples without gate have been performed to study the temperature dependence of $\Delta\sigma/\sigma$ in the range from 4 to 20 K. The EDMR signals decrease only slightly by a factor of 1.5 when T is increased from 4 to 20 K, again in agreement with Eq. (9).

From a comparison of the absolute values of $\Delta\sigma/\sigma$ as predicted by Eq. (9) and as experimentally observed, we can obtain an estimate for the differences in the scattering cross sections Σ_s and Σ_t and of the ratio of τ_e to τ_t . For X-band EDMR of a $g = 2$ resonance, $H_0 \cong 0.33$ T. Taking $m^* = 0.19m_0$ as the conduction-band transversal mass, and $n_e \cong 4 \times 10^{11} \text{ cm}^{-2}$ for the Si/SiGe heterostructure without gate, we obtain $(g \mu_B H_0 m^* / n_e \pi \hbar^2)^2 = 6 \times 10^{-5}$. Extrapolating from the power dependence shown in Fig. 4, we find an experimental value of $\Delta\sigma/\sigma \approx 10^{-5}$ for saturation ($s_e = 1$). This allows us to estimate that $\beta(\tau_t/\tau_e) \approx -1/6$. Since β can only be in the range of $0 \geq \beta \geq -1/3$, with $\beta = -1/3$ when $\Sigma_t \gg \Sigma_s$, we find that $\tau_e < 2\tau_t$. This is in accordance with earlier measurements of the single-particle relaxation rate τ_s , which was found to be typically a factor of 10 smaller than τ_t in the samples investigated here.¹

It is at first surprising that electron-electron scattering has an effect on transport measurements, since elastic electron-electron scattering does not change the total momentum of the electron gas. However, as already noted, the strong dependence of μ on n_e ($\mu \propto n_e^{2.44}$) indicates the known deviation of our sample from the behavior of an ideal 2D gas due to electron-localization effects. For (weakly) localized electrons, electron-electron scattering is not necessarily elastic because of the stronger electron-lattice coupling, and thus changes in conductivity could be expected for this scattering channel. Another possible explanation can be found considering that the 2D electronic states near the Fermi energy have different mobilities, which can lead to changes in the total mobility upon energy redistribution due to a scattering event. However, further investigations are necessary to understand the exact mechanism underlying the EDMR observed here, in particular the relationship between τ_e and τ_s .

B. g factor

According to standard kp theory, the g factor is influenced by the coupling of the electron spin to the complete band structure of the material, in particular to the valence bands and their spin-orbit splitting. In the case studied here, the electrons additionally form a quasi-2D system, in which quantum confinement plays a fundamental role. The g -factor anisotropy and the $1/n_e^2$ dependence of the signal intensity indicate that the results presented here have indeed been obtained on a quasi-2D electron system, so that the g factors found can be used for a first assessment of the influence of quantum confinement on the electron-spin properties in the low-magnetic-field limit.

TABLE I. Isotropic g factor of conduction electrons g_{ce} , and $g_{\parallel} - g_{\perp}$, as observed for Si-based samples.

| Experiment | Sample | g_{ce} | $\Delta g = g_{\parallel} - g_{\perp}$ | Ref. |
|------------|--------------------|---------------------|--|--------------|
| ESR | Si:Sb under stress | 1.9986 ± 0.0001 | 0.0011 ± 0.00005 | 27 |
| ESR | Si/SiC | 1.9993 ± 0.0001 | – | 7 |
| ESR | Si-MOSFET | 1.9988 ± 0.0001 | – | 6 |
| EDMR | Si-MOSFET | 2.000 ± 0.001 | – | 22 |
| ODMR | Si/SiGe | 1.9986 ± 0.0002 | – | 14 |
| ESR | Si/SiGe | 2.0000 ± 0.0010 | – | 9 |
| EDMR | Si/SiGe, no gate | 2.0002 ± 0.0001 | 0.0008 ± 0.0002 | Present work |

Table I shows a compilation of the isotropic g factors g_{ce} of several Si-based systems including Si:Sb under uniaxial stress, and quasi-2D systems in heterostructures as obtained from different magnetic resonance techniques. In bulk Si, $g_{ce} = 1.9987$, while g_{ce} varies from 1.9986 to 2.0002 in quantum-confined systems. Although detectable, the influence of quantum confinement on g_{ce} is small. This is due to the small spin-orbit coupling in Si, which causes the g -factor shift to be dominated by deep core levels that are less influenced by the confinement.

The differences in g_{ce} observed in the various quantum-confined systems are most likely due to their different microscopic structure, including the presence of other group-IV atoms and dopants. As an example, the g factor observed in ESR studies of Si/SiC heterostructures has possibly been influenced by the presence of P in the doping layers at a distance of 3 nm from the quantum well, which is also detected directly via its characteristic hyperfine lines.⁷ The spin-resonance techniques used are also probing the spin system in a different manner, which could lead to additional changes in the observed properties of the spin system. In fact, ODMR gives the lowest g factor, while EDMR gives the highest value, independent of the sample structure. Assuming a (slight) distribution of g factors in the constant density of states occupied by electrons in a 2D gas, ESR, ODMR, and EDMR will probe the distribution in different ways. In a very simple picture, in EDMR the most mobile electrons are the ones responsible for the electrical conduction, thus contributing to the EDMR signal. In this case, the g factor should be closer to g_0 , when compared to ESR or ODMR. On the other hand, ODMR probes electrons participating in the recombination process, i.e., electrons at the bottom of the conduction band. However, to resolve this point, comparative ESR, ODMR, and EDMR experiments have to be performed on the same heterostructures.

Concerning g -factor anisotropy, only the present work reports such an effect in a 2D electron gas in a Si-based structure. As discussed above, the experimentally observed anisotropy for high electron sheet concentrations is as expected, due to the occupation of the $\Delta(2)$ valleys only. Surprisingly, the anisotropy disappears when the electron density in the channel is lowered, and g_{ce} increases slightly in this case. There are several mechanisms that could, in principle, account for such a behavior sensitive to a change in n_e . From self-consistent calculations it was found that, as n_e increases, the average distance of the electrons from the interface decreases from about 4 to 2 nm.²² Therefore, if a gradient in stress would be present, on average the electrons would experience a different average strain level as n_e

changes. The second mechanism depending to n_e would be the contribution of a Ge-like character to the electron wave function as the average distance to the interface decreases. This Ge-like character could originate either from the Ge atoms in the SiGe barrier or from the few Ge atoms also present in the Si quantum well near the barrier. The effect would be a decrease of the g factor³⁹ with increasing n_e , and could explain the low values for $g_{\perp}[100]$ for the highest n_e studied. The third mechanism would be many-body effects, which for high magnetic fields are responsible for appreciable g shifts.⁴⁰ However, the most likely mechanism could be linked to the weak localization itself. In this model, localized electrons (dominant at low n_e) have an isotropic g factor nearer to g_0 , i.e., a more defectlike g factor, while only the delocalized electrons show the behavior expected for conduction-band electrons in silicon. We would like to point out that Wallace and Silsbee⁶ observed a g -factor increase with increasing n_e , in contrast to our results. Again, more systematic studies are necessary to resolve this point.

C. Line shape and spin relaxation

The subject of resonance linewidths and spin-relaxation phenomena has been studied extensively in solids. On the other hand, in the case of a quasi-2D electron gases very little has been done so far. Here, we would like to notice that in an EDMR experiment, in addition to the spin-relaxation mechanisms normally described in a ESR experiment, the electron transport relaxation time can play a fundamental role, thus increasing the complexity of the problem. It is clear from Figs. 3 and 8 that the linewidth is not isotropic as well, as a function of the electron density inside the channel. The n_e dependence of ΔH_{pp} is explicitly shown in Fig. 11.

Notice that the linewidth systematically increases as the angle θ between the $[100]$ growth direction and the H_0 direction increases. Jantsch *et al.*⁹ linked this behavior to the fluctuations of the Rashba field, a pseudomagnetic field caused by the lack of mirror symmetry in the quantum well used in this study (see also Ref. 41). At least two alternative explanations can also qualitatively account for such a behavior. In the first model, we assume that T_2 is determined by the spin-orbit coupling. Therefore, T_2 should decrease with an increasing deviation of the observed g factor from the value of the free electron $g_0 \approx 2.0023$. Indeed, Fig. 3 shows that the linewidth [which is proportional to $1/T_2$ according to Eq. (3)] increases for increasing $|g_0 - g|$.

Another possible relaxation mechanism responsible for the broadening is increased scattering due to interface roughness. Cyclotron orbits in the heterostructure can only exist in

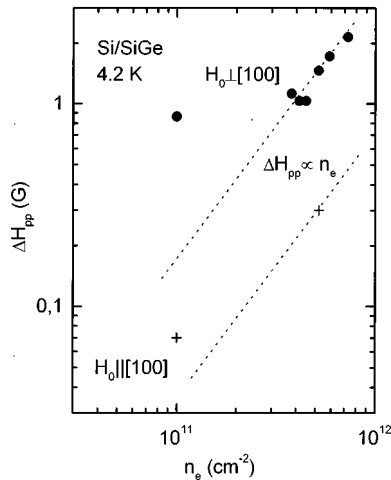


FIG. 11. EDMR linewidth ΔH_{pp} as a function of electron density n_e in the channel for the magnetic field H_0 parallel and perpendicular to the sample growth direction [100].

the plane of the 2D gas. Changing the external magnetic field from parallel to the growth direction to perpendicular leads to a reduction of the magnetic-field component perpendicular to the plane of the gas, and therefore to an increase in the electron orbit. Therefore, a larger volume of the sample can contribute to scattering, which leads to a decrease in T_2 and the observed increase in ΔH_{pp} .

As can be observed in Fig. 11, ΔH_{pp} is roughly proportional to n_e . This result could easily be understood with the help of the Drude model in 3D electron gases under the assumption, that the EDMR signal arises from electron-electron scattering. In this case, $T_2 \propto n_e^{-1}$ (Ref. 42). However, this is at variance with the predictions of Fukuyama and Abrahams for 2D electron gases; they predicted that $\tau_e \propto n_e \ln^{-1}(n_e)$. The n_e dependence of ΔH_{pp} has also been observed in Si-MOSFET quasi-2D electron-gas systems. In

ESR, Wallace and Silsbee⁶ observed that ΔH_{pp} increases with n_e , while Ghosh and Silsbee²² observed a decrease of ΔH_{pp} in EDMR. In the latter case, two spin systems contributed to the line shape, the conduction spins, and the impurity spins, thus making the data analysis more complicated.

V. CONCLUSIONS

We have presented results of electrically detected magnetic resonance in Si/SiGe quantum-well samples. The origin of the signal is assigned to spin-dependent electron-electron scattering processes. It is demonstrated that a simple model considering the polarization induced by the external magnetic field, combined with a scattering cross section dependent on the relative spin orientation, can quantitatively describe the resonant changes of the conductivity observed. The resonance is found to be anisotropic with respect to the magnetic-field orientation, in good agreement with results obtained previously on strained bulk Si. The g factor and line shape have been analyzed. However, more details concerning the relationship of the electron-electron scattering time τ_e responsible for the EDMR signal, the transverse and longitudinal spin relaxation times T_1 and T_2 , and the transport relaxation time τ_t should be addressed in future work, which could provide additional insight into the transport processes in these two-dimensional electron gases.

ACKNOWLEDGMENTS

The authors would like to thank A. Zrenner for helpful discussions and self-consistent calculations of the one electron density of states in Si/SiGe heterostructures. C.F.O.G. is pleased to acknowledge partial support from the Alexander von Humboldt Stiftung (Germany), FAPESP (Brazil), and CNPq (Brazil). The work at the Walter Schottky Institut is supported by the Deutsche Forschungsgemeinschaft (Sonderforschungsbereich 348).

*Electronic address: cfograeff@ffclrp.usp.br

¹D. Többen, F. Schäffler, A. Zrenner, and G. Abstreiter, Phys. Rev. B **46**, 4344 (1992).

²D. Monroe, Y. H. Xie, E. A. Fitzgerald, and P. J. Silverman, Phys. Rev. B **46**, 7935 (1992).

³F. F. Fang, Surf. Science **305**, 301 (1994).

⁴F. Schäffler, Semicond. Sci. Technol. **12**, 1515 (1997).

⁵K. Ismail, F. K. LeGoues, K. L. Saenger, M. Arafa, J. O. Chu, P. M. Mooney, and B. S. Meyerson, Phys. Rev. Lett. **73**, 3447 (1994).

⁶W. J. Wallace and R. H. Silsbee, Phys. Rev. B **44**, 12 964 (1991); Comment by A. Stesmans, *ibid.* **47**, 13 906 (1993); Reply by R. H. Silsbee and W. J. Wallace, *ibid.* **47**, 13 909 (1993).

⁷N. Nestle, G. Denninger, M. Vidal, C. Weinzierl, K. Brunner, K. Eberl, and K. von Klitzing, Phys. Rev. B **56**, 4359 (1997).

⁸W. Jantsch, Z. Wilamowski, N. Sandersfeld, and F. Schäffler, Phys. Status Solid. B **210**, 643 (1998).

⁹W. Jantsch, Z. Wilamowski, N. Sandersfeld, and F. Schäffler (unpublished).

¹⁰D. Stein, K. von Klitzing, and G. Weimann, Phys. Rev. Lett. **51**, 130 (1983).

¹¹M. Krapf, G. Denninger, H. Pascher, G. Weimann, and W.

Schlapp, Solid State Commun. **74**, 1141 (1990).

¹²B. Kowalski, P. Omling, B. K. Meyer, D. M. Hofmann, C. Wetzel, V. Härle, F. Scholz, and P. Sobkowicz, Phys. Rev. B **49**, 14 786 (1994).

¹³E. Glaser, J. M. Trombetta, T. A. Kennedy, S. M. Prokes, O. J. Glembocki, K. L. Wang, and C. H. Chern, Phys. Rev. Lett. **65**, 1247 (1990).

¹⁴E. R. Glaser, J. M. Trombetta, T. A. Kennedy, S. M. Prokes, O. J. Glembocki, K. L. Wang, and C. H. Chern, in *20th International Conference on the Physics of Semiconductors*, edited by E. M. Anastassakic and J. D. Joannopoulos (World Scientific, Singapore, 1990), p. 885.

¹⁵E. R. Glaser, T. A. Kennedy, D. J. Godbey, P. E. Thompson, K. L. Wang, and C. H. Chern, Phys. Rev. B **47**, 1305 (1993).

¹⁶J. Schmidt and I. Solomon, C. R. Seances Acad. Sci., Ser. B **263**, 169 (1966).

¹⁷A. Honig, Phys. Rev. Lett. **17**, 186 (1966).

¹⁸H. Dersch, L. Schweizer, and J. Stuke, Phys. Rev. B **28**, 4678 (1983).

¹⁹K. Lips and W. Fuhs, J. Appl. Phys. **74**, 3993 (1993).

²⁰C. H. Seager, E. L. Venturini, and W. K. Schubert, J. Appl. Phys. **71**, 5059 (1992).

- ²¹C. F. O. Graeff, G. Kawachi, M. S. Brandt, M. Stutzmann, and M. J. Powell, *J. Non-Cryst. Solids* **198–200**, 1117 (1996).
- ²²R. N. Ghosh and R. H. Silsbee, *Phys. Rev. B* **46**, 12 508 (1992).
- ²³C. F. O. Graeff, M. Stutzmann, and M. S. Brandt, *Phys. Rev. B* **49**, 11 028 (1994).
- ²⁴Dirk Többen, Ph.D. thesis, Technische Universität München, 1995.
- ²⁵L. Colombo, R. Resta, and S. Baroni, *Phys. Rev. B* **44**, 5572 (1991).
- ²⁶C. G. Van de Walle and R. M. Martin, *Phys. Rev. B* **34**, 5621 (1986).
- ²⁷D. K. Wilson and G. Feher, *Phys. Rev.* **124**, 1068 (1961).
- ²⁸G. Feher, *Phys. Rev.* **114**, 1219 (1959).
- ²⁹E. R. Cohen and B. N. Taylor, *Rev. Mod. Phys.* **59**, 1121 (1987).
- ³⁰C. P. Poole, *Electron Spin Resonance* (Wiley, New York, 1983).
- ³¹M. Stutzmann and D. K. Biegelsen, *Phys. Rev. B* **34**, 3093 (1986).
- ³²S. Chandrasekhar, *Astrophys. J.* **100**, 176 (1944).
- ³³R. J. Elliott, *Phys. Rev.* **96**, 266 (1954).
- ³⁴M. Stutzmann, R. A. Street, C. C. Tsai, J. B. Boyce, and S. E. Ready, *J. Appl. Phys.* **66**, 569 (1989).
- ³⁵C. Malten, F. Finger, and H. Wagner, *Solid State Commun.* **99**, 503 (1996).
- ³⁶M. Stutzmann, *Z. Phys. Chem. (Munich)* **151**, 211 (1987).
- ³⁷P. E. Lindelof, J. Norregaard, and J. Hanberg, *Phys. Scr.* **T14**, 17 (1986).
- ³⁸H. Fukuyama and E. Abrahams, *Phys. Rev. B* **27**, 5976 (1983).
- ³⁹G. Feher and D. K. Wilson, *Bull. Am. Phys. Soc.* **5**, 60 (1960).
- ⁴⁰T. Ando, A. B. Fowler, and F. Stern, *Rev. Mod. Phys.* **54**, 437 (1982).
- ⁴¹Yu. L. Bychkov and E. I. Rashba, *J. Phys. C* **17**, 6039 (1984).
- ⁴²D. Pines and C. O. Slichter, *Phys. Rev.* **100**, 1014 (1955).